Journal of Nano- and Electronic Physics
Vol. 8 No 4, 04006(6pp) (2016)

Журнал нано- та електронної фізики
Том 8 № 4, 04006(6cc) (2016)

Morphological and Electrochemical Properties of the Lactose-derived Carbon Electrode Materials

I.F. Myronyuk[1], V.I. Mandzyuk[1,*], V.M. Sachko[1], R.P. Lisovsky[2], B.I. Rachiy[1]

[1] *Vasyl Stefanyk Precarpathian National University, 57, Shevchenko St., 76018 Ivano-Frankivsk, Ukraine*
[2] *G.V. Kurdyumov Institute for Metal Physics of the NASU, 36, Academician Vernadsky Blvd., 03680 Kyiv, Ukraine*

(Received 06 June 2016; published online 03 October 2016)

The article explores the morphological and electrochemical properties of carbon electrode materials derived from D-lactose by mixing the carbon precursor with an activating reagent selected from the series KOH, K_2CO_3, $ZnCl_2$, $SnCl_2{\cdot}2H_2O$ and calcining the composite mixture at 800 °C. After dissolution and removal of K_2O, ZnO or SnO from volume of prototypes, the specific surface of carbon materials increases 1.7-4.2 times, and the electrical conductivity – 1.4-2.8 times. The activating reagents for effective influence on the properties of carbon structures can be placed in the following order: $ZnCl_2$ > KOH > K_2CO_3 > $SnCl_2{\cdot}2H_2O$. It is established that the highest specific capacity as an electrode material for supercapacitor has a sample with the highest electrical conductivity (78 $Ohm^{-1}{\cdot}m^{-1}$) obtained using KOH activating reagent. The electrode material capacity was 176-157 $F{\cdot}g^{-1}$ at discharge currents of 10-100 mA. It is found that the difference in the values of capacity of prototypes is caused by different chemical state of their surface.

Keywords: Porous carbon material, Thermochemical activation, Specific surface, Specific conductivity, Electrochemical capacitor.

DOI: 10.21272/jnep.8(4(1)).04006 PACS numbers: 61.43.Gt, 81.05.Uw, 82.47.Uv

1. INTRODUCTION

Various porous materials, in particular, metal oxides (RnO_2, IrO_2), foamed metals, individual polymers and carbon form a double electric layer (DEL) at the boundary with the electrolyte [1]. This phenomenon is the basis of the operation of new devices – electrochemical capacitors (EC), which have a high capacity and are capable of charging and discharging like secondary galvanic power sources [1-4]. Another name of these devices is supercapacitors or ionistors [5, 6]. Compared with galvanic batteries, EC have higher specific power and are significantly more durable, i.e. they endure a million charging/discharging cycles, but inferior to their specific energy.

In modern EC, porous carbon material (CM) has found widespread use as an electrode material [3, 4, 7]. This is due to its large specific surface (> 2000 m^2/g), chemical inertness relative to proton and aprotic electrolytes, simple production technology and low cost.

Currently, the choice of electrode materials for supercapacitors has significantly expanded. This is caused by the use of a wide range of organic compounds and natural raw materials for the production of CM and the invention of new methods of activation of carbon structures in order to increase their specific surface and optimize the structural and morphological characteristics.

In particular, the methods of exo- and endo-templating are used to obtain spatially ordered porous CM [3, 4, 6-12]. The first method involves thermolytic decomposition of the carbon precursor in the pore volume of inorganic matrices – zeolites [13-15], silica molecular sieves or alumina membranes [16-19]. The voids of exo-templates as a result of carbonization of the organic matter become the carbon frame, and a free volume in the form of pores and channels appears in place of the matrix after its dissolution and removal. The essence of the endo-templating method is that the volume of the carbon precursor is filled with nanoparticles of inorganic oxide material (for example, SiO_2 and Al_2O_3), and after carbonization of the precursor, they are washed out from CM by KOH solution, fluoride or chloride acid [20-22].

Carbon structures with multimodal pores are the most suitable for the production of EC electrodes. Since micropores make the greatest contribution to the specific CM surface, their share in the total volume of the material pores always exceeds the share of meso- and macropores. The activation thermochemical processes, which lead to an increase in the micropore volume in the carbon matrix, are due to the reactive interaction of H_2O and CO_2 molecules with carbon atoms at temperatures of 800-1100 °C [23, 24]

$$C_n + H_2O = C_{n-1} + CO + H_2, \quad (1)$$

$$C_n + CO_2 = C_{n-1} + 2CO. \quad (2)$$

Carbon structures with the necessary ratio of micro- and mesopores are synthesized using activating reagents KOH, K_2CO_3 or $ZnCl_2$ [25-28]. When heated composite mixtures consisting of the carbon precursor and specified compounds, K_2O and ZnO template particles are formed, which after removal from the carbon matrix leave there 2-6 nm mesopores. H_2O and CO_2 molecules released as a result of thermal dissociation of reagents are involved in the oxidation of carbon atoms and contribute to growth of the micropore volume in the material (reactions (1), (2)). The specified compounds in the composition of the carbon precursor act as both a template and an activating reagent; therefore, they should be used when producing new electrode materials based on promising carbon precursors.

Studying the structural and morphological properties of CM obtained by thermolysis of disaccharides, in particular, sucrose and D-lactose, which have the same chemical composition (the formula of precursors $C_{12}H_{22}O_{11}$), we clarified that lactose carbon is more promising than carbon derived from sucrose for producing EC electrodes.

* mandzyuk_vova@ukr.net

This is due to the fact that the texture of lactose carbon is constructed of very small, 5.0 × 0.4 × 0.4 nm^3 layered crystallites, and the texture of sucrose carbon – largely of globular 2.4-3.0 nm microcrystals [29]. Actually, each microcrystal of lactose carbon is formed of two graphene sheets. This morphological peculiarity provides lactose carbon with a higher electrical conductivity and a much larger specific surface.

Thus, the aim of this work was to study the structural and morphological and electrochemical properties of carbon samples obtained by calcining the composite mixture of D-lactose and an activating reagent (KOH, K_2CO_3, $ZnCl_2$, $SnCl_2$) at a temperature of 800 °C and clarify how the acquired properties of carbon structures influence the capacity of EC formed on their basis.

2. PRODUCTION OF PROTOTYPES AND METHODS OF THEIR STUDY

D-lactose $C_{12}H_{22}O_{11}$ (TC 6-09-2293-77) was used as the carbon precursor. The structural and morphological properties of carbon were corrected using reagents-activators: pure KOH for the analysis (SS 24263-80), technical K_2CO_3 (SS 10690-73), pure $ZnCl_2$ for the analysis (SS 4529-78) and chemically pure $SnCl_2{\cdot}2H_2O$ (SS 36-78). To this end, D-lactose was introduced into the saturated solution of the activating reagent; then the mixture was stirred and heated in order to form a liquid homogeneous consistency. After evaporation (100-175 °C) and caramelization (220-230 °C), the composite mixture was carbonized at a temperature of 350 °C for 1 hour. After that, the carbon mixture with the reagent was heated in an argon atmosphere at 800 °C for 40-60 minutes. The conditions for obtaining CM prototypes are given in Table 1.

K_2O template particles were extracted from the volume of calcined CM with hot distilled water, and ZnO and SnO – with hot chloride acid.

The structural and morphological characteristics of CM were determined by nitrogen adsorption/desorption isotherms. The measurements were performed at the boiling point of liquefied nitrogen ($T = 77$ K) on an automatic sorptometer Quantachrome Autosorb (Nova 2200e). Before the measurements, the prototypes were calcined in vacuum at a temperature of 180 °C for 24 hours. The total specific surface of pores (S_p), the specific surface of micro- (S_{micro}) and mesopores (S_{meso}), the volume of micro- (V_{micro}) and mesopores (V_{meso}) were calculated using the BET- [30] and *t*- [31] methods. The total volume of pores (V) was determined by the amount of adsorbed nitrogen at a pressure of $p/p_0 \approx 1$ (where p and p_0 are the nitrogen vapor pressure and the pressure of its saturated vapor at a temperature of 77 K, respectively). The calculation of pore size distribution was carried out by the NLDFT (nonlocal density functional theory) method [32] in the approximation of slit-like pores.

To study the conducting CM parameters, a capacitor system consisting of two copper electrodes with the prototype between them was used. The Nyquist diagrams $Z'' = f(Z')$, where Z' and Z'' are the real and imaginary parts of the complex resistance of the system, respectively, were obtained using amplitude-frequency analyzer Autolab ("ECO CHEMIE", Netherlands) in the frequency range of 10^{-2}-10^5 Hz. The amplitude of the sinusoidal voltage was equal to 10 mV. Taking into account the geometric parameters of the samples, the specific values of the resistances, electrical conductivity and frequency dependences of the electrical parameters were calculated according to the following equations:

$$\rho^* = \rho' - j\rho'', \tag{3}$$

where $\rho' = Z'A/d$ and $\rho'' = Z''A/d$, A and d are the electrode surface area and the sample thickness, respectively. The complex specific conductivity was determined from the relationship

$$\sigma^* = 1/\rho^* = \sigma' + j\sigma'', \tag{4}$$

where $\sigma' = \rho'/M$, $\sigma'' = \rho''/M$, $M = \left|Z^*\right|^2 \left(A/d\right)^2$, and the total conductivity – by the formula [33]

$$\sigma^* = \sqrt{\left(\sigma'\right)^2 + \left(\sigma''\right)^2}. \tag{5}$$

A mixture of CM and conductive additive (graphite KS-15 by Lonza Co.) was used in a mass ratio of 75 : 25 to produce electrodes of symmetrical EC. The obtained electrodes were impregnated with the electrolyte, separated by a separator and placed in a two-electrode cell of a standard size of 2525, after which it was sealed. 30 % KOH aqueous solution was used as the electrolyte.

Galvanostatic cycling and cyclic voltammetry were used to study the electrochemical properties of EC with electrodes based on CM prototypes. The measurements were performed on the device Autolab ("ECO CHEMIE", Netherlands) equipped with the GPES program.

The galvanostatic measurements were carried out in the voltage range of $0 \div 1$ V, the capacitor charge/discharge current varied from 10 to 100 mA with a step of 10 mA. The specific capacity of the electrode material of EC was calculated by the formula

$$C = I\,t_d / \left[2(U_m - \Delta U)m\right], \tag{6}$$

Table 1 – Conditions for obtaining the prototypes of lactose carbon

CM designation	Activating reagent	Lactose/reagent mass ratio	Activation temperature, °C	Activation duration, min
C	–	–	800	40
C_{KOH}	KOH	1:3	800	40
$C_{K_2CO_3}$	K_2CO_3	1:5	800	40
C_{ZnCl_2}	$ZnCl_2$	1:5	800	60
C_{SnCl_2}	$SnCl_2{\cdot}2H_2O$	1:5	800	60

where I is the charge/discharge current, t_d is the discharge time, U_m is the maximum voltage, ΔU is the voltage drop when the discharge circuit is closed, m is the CM mass. The internal resistance of EC was determined by a potential jump after ten charge/discharge cycles of the capacitor according to the equality $\Delta U = 2IR$.

The EC cyclic voltammograms were recorded in the voltage range of 0 ÷ 1 V; the scan rate $s = dU/dt$ was equal to 5 and 10 mV/s.

3. RESULTS AND DISCUSSION

The necessary initial information for calculating the structural and morphological characteristics of the CM prototypes is given by the experimental dependences of changes in the volume V of adsorbed/desorbed nitrogen on the value of its relative pressure p/p_0 at a constant temperature (see Fig. 1).

An important feature of the nitrogen adsorption/desorption isotherms of the prototypes is that when the saturated vapor pressure reaches p_0, the limiting value of adsorption is detected. The adsorption dependences with these features are typical for monomolecular adsorption of substances by porous sorbents. By the IUPAC classification, they belong to the I-st type [34]. The dependences shown in Fig. 1 indicate that calcining of the composite mixture of carbon with the activating reagent leads to a significant increase in the sorption properties of the prototypes. By the effectiveness of the influence on the activation process, the reagents can be arranged in the series of $ZnCl_2$ > KOH > K_2CO_3 > $SnCl_2 \cdot 2H_2O$.

To calculate the pore size distribution of the porous material, as a rule, the desorption isotherm is used and the hysteresis between adsorption and desorption dependences is taken into account. The essence of hysteresis lies in the fact that the desorption branch is shifted in the direction of lower pressure values p/p_0. The isotherm hysteresis of C_{KOH} sample is detected within the range of 0.1 ÷ 1.0 p/p_0 and of C_{ZnCl_2} sample – within the range of 0.15 ÷ 0.65 p/p_0. The shape of the hysteresis loop of these isotherms by the IUPAC classification [34] is typical for porous materials, in which slit-like pores are dominant.

As seen from the calculation of the parameters of the CM porous structure (Table 2), unactivated carbon (C) has a moderate specific surface of 499 $m^2 \cdot g^{-1}$ and a small pore volume of 0.222 $cm^3 \cdot g^{-1}$. However, as a result of the activation thermochemical processes with the participation of different reagents, the specific surface of the prototypes increases 1.7-4.2 times and the pore volume – 1.8-5.3 times. These values in the activated C_{ZnCl_2} are the largest: S_p = 2122 $m^2 \cdot g^{-1}$; V = 1.168 $cm^3\ g^{-1}$, and in the C_{SnCl_2} – the smallest: S_p = 841 $m^2 \cdot g^{-1}$; V = 0.402 $cm^3\ g^{-1}$.

There is a redistribution of micro- and mesopores in addition to the growth of S_p and V with the activation of $ZnCl_2$. If for the unactivated material S_{micro}/S_p = 92 % and V_{micro}/V = 88 %, then after activation S_{micro}/S_p = 59 % and V_{micro}/V = 45 %. For other prototypes, the dominance of micropores is typical.

The analysis of the characteristic curves of the pore volume size distribution calculated using the CM adsorption isotherms, convinces us that unactivated carbon C is really microporous (Fig. 2, curve 1). Most of its micropores has a size of 1.17 nm. In the activated prototypes C_{SnCl_2}, $C_{K_2CO_3}$ and C_{KOH}, the micropore volume is 75-91 % with respect to the total pore volume. Micropores in these prototypes have a size of 1.17-1.40 nm (Fig. 2, curves 2, 3, 5). The activated prototype C_{ZnCl_2} is special. Its total pore volume contains 45 % micropores and 55 % mesopores. In addition, the micropore sizes in the main maximum and in two smaller maxima are, respectively, equal to 1.23, 1.54 and 1.85 nm (Fig. 2, curve 4). The maxima in the mesopore distribution for this material correspond to the sizes of 2.31; 2.65 and 3.32 nm.

Table 2 – Parameters of the porous structure of electrode materials based on D-lactose

Material	S_n, m^2/g	S_{micro}, m^2/g	S_{meso}, m^2/g	V, cm^3/g	V_{micro}, cm^3/g	V_{meso}, cm^3/g
C	499	455	44	0.222	0.198	0.024
C_{KOH}	1078	1021	57	0.463	0.421	0.042
$C_{K_2CO_3}$	897	778	119	0.423	0.322	0.101
C_{ZnCl_2}	2122	1251	871	1.168	0.522	0.640
C_{SnCl_2}	841	737	104	0.402	0.303	0.099

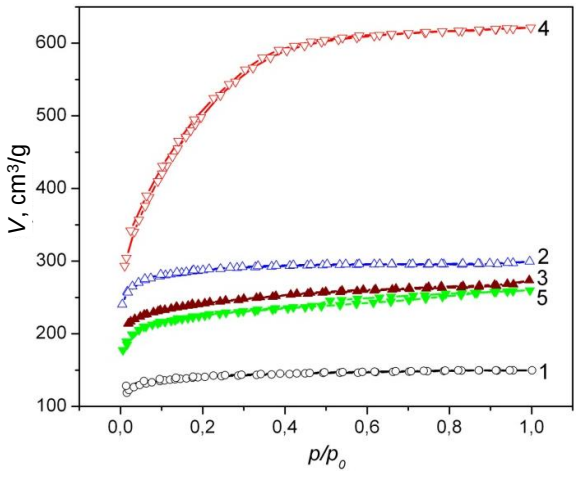

Fig. 1 – Nitrogen adsorption/desorption isotherms of CM: C (1), C_{KOH} (2), $C_{K_2CO_3}$ (3), C_{ZnCl_2} (4) and C_{SnCl_2} (5)

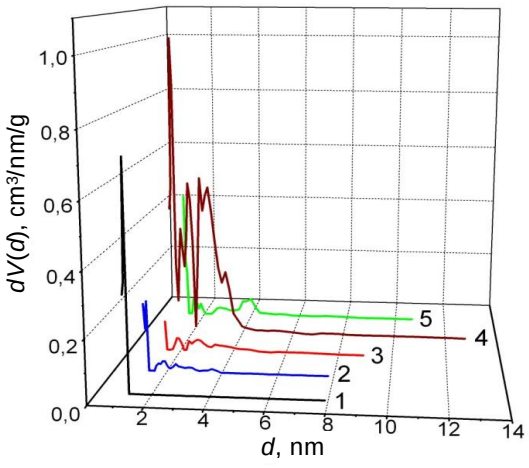

Fig. 2 – Pore size distribution in CM: C (1), C_{KOH} (2), $C_{K_2CO_3}$ (3), C_{ZnCl_2} (4) and C_{SnCl_2} (5)

Since the advantage of supercapacitors compared to galvanic batteries is precisely the ability to high current discharge; therefore, the electrode material and the EC electrolyte should have high electrical conductivity.

As seen from the Nyquist diagrams $Z'' = f(Z')$ (see Fig. 3), the inductive component is present in the high-frequency spectral region of all samples. Its presence is associated with the percolation carrier transport mechanism through a mixture of conducting and non-conducting particles of the electrode material, where pores are the non-conducting particles. Thus, due to the complex motion trajectory of charge carriers, the carbon structure of the electrode material becomes an analogue of inductance. Only the real component of the resistance undergoes changes with decreasing frequency of the electric potential. The value of the imaginary resistance first decreases, and then remains constant.

Based on the equations (3)-(5), the values of the real σ', imaginary σ'' and total σ^* conductivities of CM are calculated and their frequency dependences are found. Since the value of the real component of the electrical conductivity at frequencies below 10^3 Hz is approximately 2-3 orders of magnitude larger than the value of the imaginary component, then the contribution of the latter to the total conductivity of CM can be neglected. Under these circumstances, the behavior of the total resistance will also be determined, mainly, by the frequency dependence of the real component of the electrical conductivity.

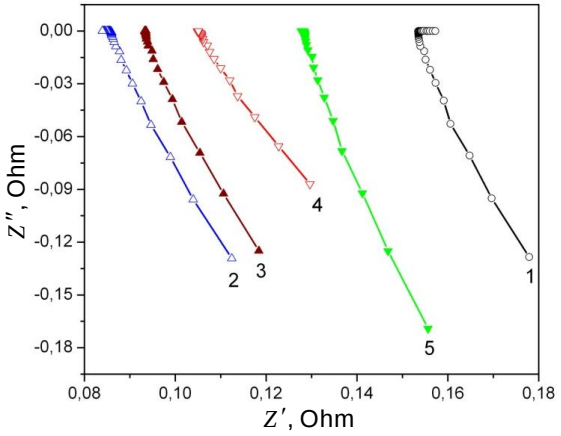

Fig. 3 – Nyquist diagrams of CM: C (1), C_{KOH} (2), $C_{K_2CO_3}$ (3), C_{ZnCl_2} (4) and C_{SnCl_2} (5)

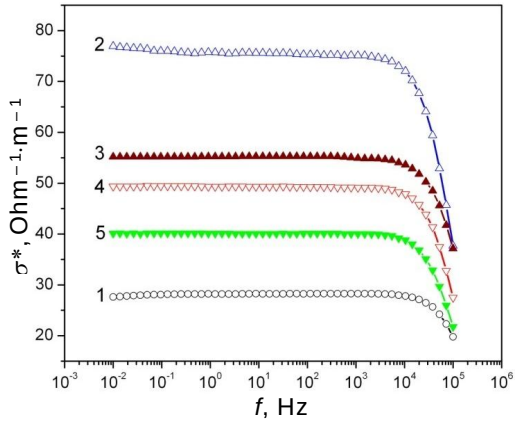

Fig. 4 – Frequency dependence of the total conductivity of CM: C (1), C_{KOH} (2), $C_{K_2CO_3}$ (3), C_{ZnCl_2} (4) and C_{SnCl_2} (5)

Representation of the frequency dependences of the electrical conductivity in semi-logarithmic coordinates allows to determine the value of the specific CM electrical conductivity by extrapolating the experimental curve to its intersection with the σ^*-axis (we have a constant current at $f \to 0$) (see Fig. 4).

The calculations performed in such a way allowed to clarify that the high-temperature activation of CM using the mentioned reagents leads to an increase in its specific conductivity 1.4 ÷ 2.8 times (see Table 3). CM C_{KOH} acquires the greatest value of the electrical conductivity (78 $Ohm^{-1} \cdot m^{-1}$) and CM $C_{K_2CO_3}$ – a somewhat smaller (55 $Ohm^{-1} \cdot m^{-1}$). Such a result of the effect of KOH and K_2CO_3 on the CM electrical conductivity, in our opinion, is associated with the intercalation of K^+ ions in the interlayer space of carbon microcrystallites. This contributes to their structural rearrangement at high temperatures to the graphite-like state.

To determine the specific energy parameters of CM, the electrodes were formed from them. On the basis of the galvanostatic curves $U = f(t)$ (Fig. 5), the values of the specific capacity of electrode materials (Fig. 6a) and the internal resistance of EC (Fig. 6b) on the discharge current were calculated.

Analyzing the curves shown in Fig. 6, it can be found that electrode material C_{KOH} exhibits the largest specific capacity (176-157 $F \cdot g^{-1}$) in a discharge with a current of 10-100 mA. The material $C_{K_2CO_3}$ has a slightly lower specific capacity (171-147 $F \cdot g^{-1}$) at the same discharge currents. It is unexpected that C_{ZnCl_2} CM with the largest values of the surface area (2122 $m^2 \cdot g^{-1}$) and micropore volume (0.522 $cm^3 \cdot g^{-1}$) shows the same specific capacity as unactivated carbon (160-135 $F \cdot g^{-1}$). By the specific capacity, the prototypes can be arranged in a series of

Table 3 – Specific electrical conductivities of CM based on D-lactose

Material	σ^*, $Ohm^{-1} \cdot m^{-1}$
C	28
C_{KOH}	78
$C_{K_2CO_3}$	55
C_{ZnCl_2}	49
C_{SnCl_2}	40

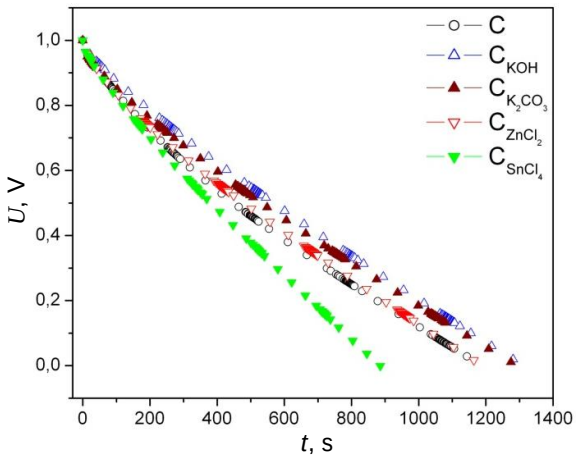

Fig. 5 – Discharge curves of EC with electrodes based on CM at a current of 10 mA

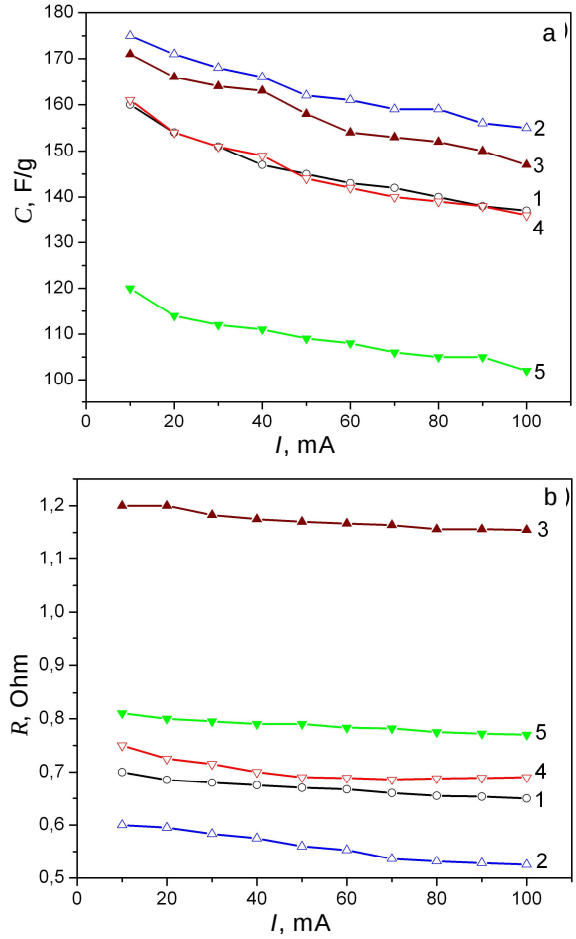

Fig. 6 – Dependences of the specific capacity (a) and internal resistance (b) on the EC discharge current with electrodes based on CM: C (1), C_{KOH} (2), $C_{K_2CO_3}$ (3), C_{ZnCl_2} (4) and C_{SnCl_2} (5)

$$C_{KOH} > C_{K_2CO_3} > C_{ZnCl_2},\ C > C_{SnCl_2}.$$

Searching for the relationship between the specific capacity of CM, the value of the internal resistance of EC and the specific conductivity of the materials themselves, it is possible to reveal the correlation correspondence only between the specific capacity and the specific conductivity of three samples C_{KOH}, $C_{K_2CO_3}$ and C_{ZnCl_2}. Experimental results do not allow to detect a direct effect of the morphological parameters of the porous structure of CM on their electrochemical properties. In particular, there is no clear correspondence between the value of the specific capacity of the electrode material and its specific surface. This indicates a significant effect on the formation of DEL of the chemical state of the surface of carbon structures. Among the studied materials, only the surface of carbon C_{KOH} is most closely related to the electrolyte KOH. First of all, the possibility of forming DEL micelles on the surface of CM is meant by the term "affinity of the electrolyte to the electrode material". In this heterogeneous system, the formation of micelles is possible in the case of the hydroxylation of the electrode material surface. The prototype C_{KOH} acquires the hydroxylation state in the process of the reaction interaction with the activating reagent:

$$C_n + 4KOH = C_{n-2}(COH) + 2K_2O + CO + \frac{3}{2}H_2. \quad (7)$$

As a result of this reaction, there occurs an increase in the CM microporosity and the formation of $\equiv C-OH$ surface groups. A micellar $\{m[C(C\text{-}O)]nK^+(n\text{-}x)OH^-\}^{x+}xOH$ DEL, in which the K^+ ions are potential-determining, is formed on the hydroxylated surface of the electrode CM when in contact with alkaline electrolyte. The use of the activating reagents K_2CO_3, $ZnCl_2$, $SnCl_2{\cdot}2H_2O$ also provides an increase in the porosity of carbon samples, however, the chemical state of their surface is less suitable for the formation of DEL in the electrolyte, since groups compensating the surface charge are formed:

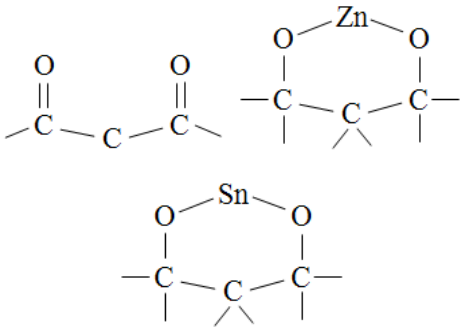

Based on the cyclic voltammetry data taken at a lower scan rate (5 mV/s), the voltammograms have a symmetrical shape similar to the rectangular one (Fig. 7a).

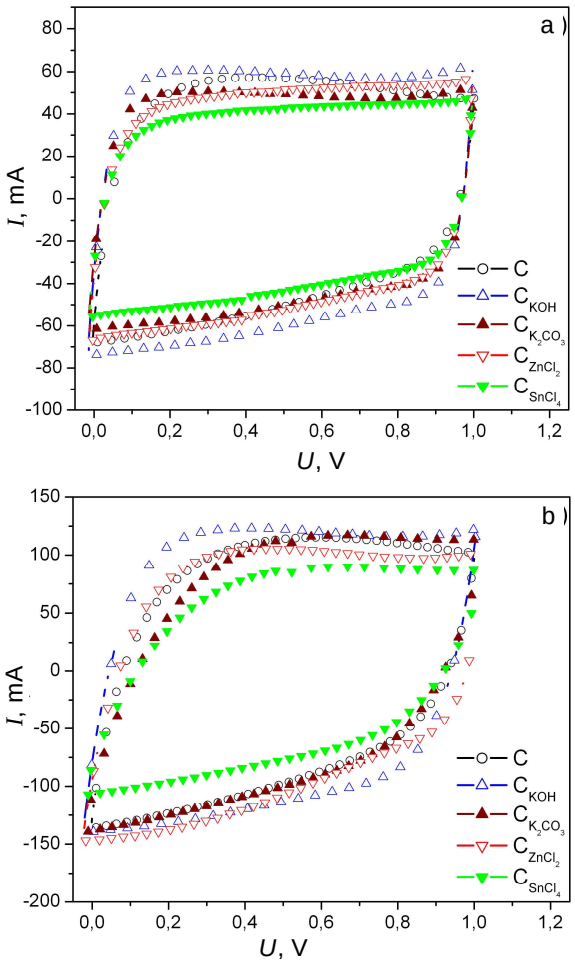

Fig. 7 – Cyclic voltammograms of EC taken at a scan rate of 5 mV/s (a) and 10 mV/s (b)

Such a shape of the voltammograms implies that the charge accumulation in EC occurs precisely as a result of the DEL formation at the interface between the electrode material and the electrolyte; and there are no secondary oxidation-reduction, the so-called Faraday, processes. At a higher scan rate (10 mV/s), the rectangular shape of the voltammograms is slightly disturbed (Fig. 7b). This is caused by an increase in the resistance of the electrochemical system due to a local decrease in the concentration of electrolyte ions in the micropores of the electron material [35].

4. CONCLUSIONS

A method for producing a synthetic CM based on the use of D-lactose as a precursor and also an activating reagent selected from the KOH, K_2CO_3, $ZnCl_2$, $SnCl_2{\cdot}2H_2O$ series is proposed. It involves mixing the precursor with an activating reagent and heating the composite mixture first to the carbonization temperature of the organic component (350 °C), and then to a temperature of 800 °C, at which there occurs the activation processes, namely, an increase in the pore volume, an increase in the specific surface of the material, as well as the atomic structure ordering of graphene microcrystals.

Studies of the structural and morphological state and the electrical conductivity of CM showed that after their thermochemical activation, the pore volume and the specific surface of the material increase, respectively, 1.8-5.3 and 1.7-4.2 times, and the specific electrical conductivity – 1.4-2.8 times. By the effectiveness of the effect on the CM properties, the activating reagents can be arranged in the series of $ZnCl_2$ > KOH > K_2CO_3 > $SnCl_2{\cdot}2H_2O$.

As the electrode material for EC, the largest specific capacity is demonstrated by the CM with the highest specific electrical conductivity and activated by the KOH reagent. When discharging EC with currents of 10-100 mA, the specific capacity of the electrode material is equal to 176-157 $F{\cdot}g^{-1}$. Although the material activated by $ZnCl_2$ possesses the greatest values of the micropore volume (0.522 $cm^3{\cdot}g^{-1}$) and the specific surface (2122 $m^2{\cdot}g^{-1}$), it shows the same specific capacity as unactivated carbon (160-135 $F{\cdot}g^{-1}$). The difference in the values of the specific capacity of the studied electrode materials is associated with different chemical states of their surface.

REFERENCES

1. B.E. Conway, *Electrochemical supercapacitors. Scientific fundamentals and technological applications* (N. Y.: Kluwer Academic/Plenum Publ.: 1999).
2. E. Frackowiak, F. Beguin, *Carbon* 39 No 6, 937 (2001).
3. F. Beguin, E. Frackowiak. *Carbons for Electrochemical Energy Storage and Conversion Systems* (Boca Raton, FL: CRC Press: 2010).
4. Yu.M. Volfkovych, T.M. Serdyuk, *Elektrokhimiya* 38 No 9, 1043 (2002).
5. B.K. Ostafiychuk, I.M. Budzulyak, M.M. Kuzyshyn, B.I. Rachiy, R.A. Zatorskyy, R.P. Lisovskyy, V.I. Mandzyuk, *J. Nano-Electron. Phys.* 5 No 3, 03049 (2013).
6. B.I. Rachiy, B.K. Ostafiychuk, I.M. Budzulyak, V.M. Vashchinskiy, R.P. Lisovskiy, V.I. Mandzyuk, *J. Nano- Electron. Phys.* 6 No 4, 04031 (2014).
7. W. Gu, G. Yushin, *WIREs Energy Environ.* 3 No 5, 424 (2014).
8. N.D. Shcherban, V.H. Il'yin, *Khimiya, fizyka ta tekhnolohiya poverkhni* 6 No 1, 97 (2015).
9. B. Sakintuna, Y. Yürüm, *Ind. Eng. Chem. Res.* 44 No 9, 2893 (2005).
10. R. Ryoo, S.H. Joo, S. Jun, *J. Phys. Chem. B* 103 No 37, 7743 (1999).
11. C. Liang, S. Dai, *J. Am. Chem. Soc.* 128 No 16, 5316 (2006).
12. S.B. Yoon, J.Y. Kim, J.S. Yu, *Chem. Commun.* 14, 1536 (2002).
13. T. Kyotani, Z. Ma, A. Tomita, *Carbon* 41 No 7, 1451 (2003).
14. J. Rodriguez-Mirasol, I. Cordero, L.R. Radovic, J.J. Rodriguez, *Chem. Mater.* 10 No 2, 550 (1998).
15. Z. Ma, T. Kyotani, A. Tomita, *Chem. Commun.* 23, 2365 (2000).
16. S. Jun, S.H. Joo, R. Ryoo, M. Kruk, M. Jaroniec, Z. Liu, T. Ohsuna, O. Terasaki, *J. Am. Chem. Soc.* 122 No 43, 10712 (2000).
17. Y. Xia, Z. Yang, R. Mokaya, *J. Phys. Chem. B* 108 No 50, 19293 (2004).
18. A. Lu, A. Kiefer, W. Schmidt, F. Schüth, *Chem. Mater.* 16 No 1, 100 (2004).
19. S. Alvarez, A.B. Fuertes, *Carbon* 42 No 2, 433 (2004).
20. J. Jang, B. Lim, *Adv. Mater.* 14 No 19, 1390 (2002).
21. S.B. Yoon, G.S. Chai, S.K. Kang, J.S. Yu, K.P. Gierszal, M. Jaroniec, *J. Am. Chem. Soc.* 127 No 12, 4188 (2005).
22. T. Kyotani, L.F. Tsai, A. Tomita, *Chem. Mat.* 7, 1427 (1995).
23. H. Nakagawa, A. Shudo, K. Miura, *J. Electrochem. Soc.* 147, 38 (2000).
24. S. Román, J.F. González, C.M. González-García, F. Zamora, *Fuel Proc. Tech.* 89, 715 (2008).
25. A.P. Carvalho, M. Gomes, A.S. Mestre, M. Brotas de Carvalho, *Carbon* 42 No 3, 672 (2004).
26. J. Hayashi, M. Uchibayashi, T. Horikawa, K. Muroyama, V.G. Gomes, *Carbon* 40 No 15, 2747 (2002).
27. M. Molina-Sabio, F. Rodriguez-Reinoso, *Colloids Surf. A* 241 No 1, 15 (2004).
28. S. Yorgun, N. Vural, H. Demiral, *Microporous Mesoporous Mater.* 122 No 1, 189 (2009).
29. I.F. Myronyuk, V.I. Mandzyuk, V.M. Sachko, Yu.O. Kulyk, *Phys. Chem. Solid State* 16 No 4, 700 (2015).
30. A. Adamson, *Fizicheskaya khimiya poverkhnostey* (Moskva: Mir: 1979).
31. D. Lozano-Castelló, F. Suárez-Garsía, D. Cazorla-Amorós, Á. Linares-Solano, *Porous texture of carbons* in *Carbons for Electrochemical Energy Storage Systems* (F. Béguin and E. Frackowiak, Boca Raton-New York: CRC Press - Taylor and Francis Group: 2002).
32. A.V. Neimark, P.I. Ravikovitch, *Microporous Mesoporous Mater.* 44/45, 697 (2001).
33. M.H. Abdullah, A.N. Yusoff, *J. Alloy. Compd.* 233, 129 (1996).
34. S.J. Gregg, K.S.W. Sing, *Adsorption, surface area and porosity* (2nd ed. London: Academic Press: 1982).
35. H. Wang, L. Pilon, *Electrochim. Acta* 64, 130 (2012).